Functional Materials 16, No.2 (2009)

The local charge carrier interaction with lattice defects in ZnCdTe and ZnHgTe solid solutions

O.P.Malyk

Lviv Polytechnical National University, Semiconductor Electronics Department, 12 Bandera Street, 79013 Lviv, Ukraine

Received December 23, 2008

The processes of the charge carrier scattering on the short-range potential caused by interaction with polar and nonpolar optical phonons, piezoelectric and acoustic phonons, static strain, neutral and ionized impurities in $Zn_xCd_{1-x}Te$ ($0 \le x \le 1$) and $Zn_xHg_{1-x}Te$ ($x = 0.15$) are considered. The temperature dependence of the charge carrier mobility in temperature range 50–360 K are calculated.

Рассмотрены процессы рассеяния носителя заряда на близко-действующем потенциале, вызванном взаимодействием с полярным и неполярным оптическими фононами, пьезоэлектрическими и акустическими фононами, статической деформацией, нейтральными и ионизированными примесями в $Zn_xCd_{1-x}Te$ ($0 \le x \le 1$) и $Zn_xHg_{1-x}Te$ ($x = 0.15$). Рассчитаны температурные зависимости подвижности носителя заряда в интервале температур 50–360 К.

The solid solution $Zn_xCd_{1-x}Te$ is regarded as one of the most promising materials for radiation detectors operated at room temperature [1]. However, as far as we know, the dominant scattering mechanisms for carrier transport and their temperature dependences are not well known for CdZnTe system [2–5]. Moreover, the solid solution $Zn_xHg_{1-x}Te$ is considered as a potentially superior infrared detector material due to its better stability as compared to HgCdTe alloy [6–10]. The common feature of the transport phenomena description in these solutions is the use of the long-range charge carrier scattering models. In such models, it is supposed that either charge carrier interacts with the whole crystal (electron-phonon interaction) or it interacts with the impurity defect potential having the action radius of ~50–100a_0 (a_0 is the lattice constant). However, such an assumption contradicts the special relativity theory according to which the charge carrier should interact only with the neighbouring crystal region. Besides, for defects with interaction energy $U \approx 1/r^n$ ($n = 1,2$) on distances ~10a_0, the potential becomes the magnitude of the second order infinitesimal, while all theories mentioned above are considered under the first (Born) approximation. On the other side, the short-range models of electron scattering in $Cd_xHg_{1-x}Te$ and $Cd_xHg_{1-x}Se$ were proposed [11, 12] free of the above drawbacks. There it has been supposed that the carrier interact with the defect potential only within one unit cell. The purpose of this work is to use this approach to describe the carrier scattering processes on the various types of crystal defects in CdZnTe and ZnHgTe solid solutions.

For the charge carrier scattering on the nonpolar optical (NPO) and acoustic (AC) phonons, static strain (SS) centers, disorder (DIS) potentials and neutral (NI) defects, the interaction radius of the short-range potential was limited by one unit cell. For the carrier scattering on the ionized impurities (II), polar optical (PO) and piezoelectric

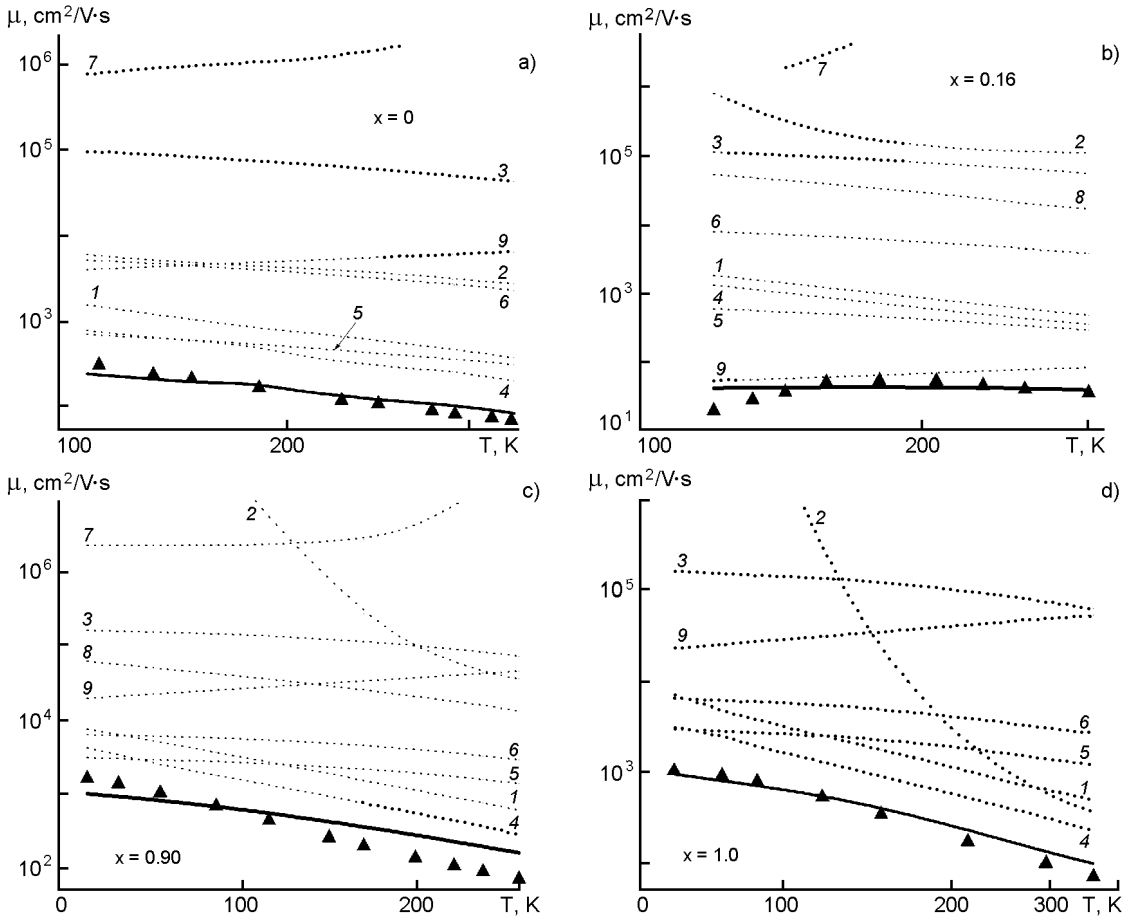

Fig. 1. Temperature dependencеы of heavy-hole mobility in $Zn_xCd_{1-x}Te$ crystals. Solid line, mixed scattering mode; *1*, *2*, *3*, *4*, *5*, *6*, *7*, *8*, *9*, AC, II, NPO, PAC, PO, POP, NEU, DIS, SS scattering mode, respectively. Experimental data from [2, 15, 16].

(piezoacoustic (PAC) and piezooptic (POP)) phonons, the interaction radius of the short-range potential was found in a form $R = \gamma a$ (a is the lattice constant; γ, the respective adjustable parameter). It is to nite that the heavy power dependence of parameters γ_{PO}, γ_{PZ}, γ_{II} limits sharply the choice opportunities of their numerical values. The respective charge carrier transition probability from state k to state k' caused by the interaction with defect potential was determined according to [11, 12]. To describe the charge carrier scattering on a disorder potential, the respective transition probability determined in [13] was used.

The calculation of the conductivity tensor components were calculated basing on the formalism of the exact solution of the stationary Boltzmann equation [14]. Using this formalism, an additional adjustable parameter $\gamma_{SS}N_{SS}$ for SS-scattering mode can be obtained.

The theoretical temperature dependences of the heavy-hole mobility were compared with the experimental data presented in [2, 15, 16] for $Zn_xCd_{1-x}Te$ crystals with compositions $x = 0$ (sample A-71 [15]), $x = 0.16$, 0.90, and $x = 1$ (Ag — doped sample [16]). For $0<x<1$, the Fermi level was obtained from the electroneutrality equation:

$$p \approx N_A\left[2\exp\left(\frac{E_A - E_F}{k_BT}\right) + 1\right]^{-1},$$

where E_A is the acceptor ionization energy determined in [2]; N_A, the acceptor concentration obtained from the composition dependence of hole concentration at 300 K (see Fig. 4 in [2]). For $x = 0$, the neutrality equation looks like:

$$p \approx N_A\left[2\exp\left(\frac{E_A - E_F}{k_B T}\right) + 1\right]^{-1} - N_D,$$

where E_A, N_A, $NIVD$ ($NIVD$ is the donor concentration) determined in [15]. For $x = 1$, the Fermi level was obtained from equation $p = N_A^+ = 1/eR$, R being the experimental Hall coefficient value determined in [16].

The theoretical $\mu(T)$ curves for $Zn_xCd_{1-x}Te$ are presented in Fig. 1a–d. The solid lines represent the curves calculated basing on the short-range models within the framework of the exact solution of the Boltzmann equation. The obtained scattering parameters for different scattering modes are listed in Table. It is seen that the theoretical curves agree well with experimental data in the whole investigated temperature range. To estimate the role of the different scattering mechanisms, the appropriate dependences are presented in Fig. 1a–d by the dotted lines.

It is seen that at the Cd-rich side, the main scattering mechanisms are static strain, polar optical, acoustic and piezoacoustic scattering. The low contribution of SS-scattering for $x = 0$ can be explained by an improved quality of the crystal as compared to the case $x > 0$. In the low temperature region, the different slope of the theoretical curve and the experimental data is observed. It can be explained by the incompleteness of the SS-scattering model where the angular dependence of interaction potential must be taken into account.

At the Zn-rich side, the polar optical, acoustic, and piezoacoustic mechanisms are the dominant scattering mechanisms, too. In this case, the influence of the SS-scattering is less substantial. Other scattering mechanisms such as ionized and neutral impurity scattering, piezooptic and nonpolar optical phonon scattering, disorder scattering give negligibly small contributions.

Table. Parameters γ for different scattering modes

x	γ_{PO}	γ_{II}	γ_{PZ}	γ_{SS} $N_{SS}\times10^{-14}$, cm^{-3}
ZnCdTe				
0.00	0.44	1.0	0.34	0.50
0.16	0.45	1.0	0.33	40.0
0.80	0.40	1.0	0.37	0.10
1.00	0.39	1.0	0.35	0.10
ZnHgTe				
0.15	0.70	1.0	0.55	70.0

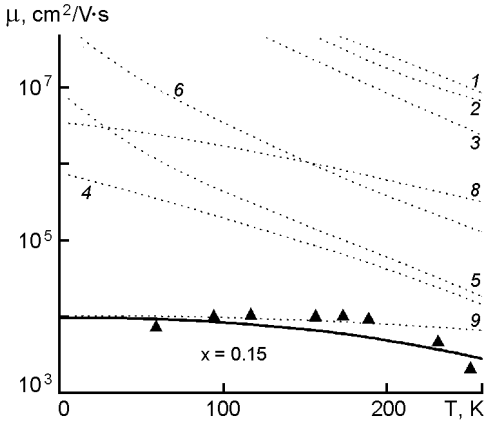

Fig. 2. Temperature dependences of the electron mobility in $Zn_xHg_{1-x}Te$ crystal. Curve notations the same as in Fig. 1. Experimental data are taken from [6].

For $Zn_xHg_{1-x}Te$ ($x = 0.15$) crystal a comparison of the theoretical temperature dependences of the electron mobility was made with the experimental data presented in [6]. The Fermi level was obtained from equation $n = 1/eR$, R being the experimental value of the Hall coefficient determined in [6]. It is seen from Fig. 2 that the static strain, the piezoacoustic and the polar optical mechanisms are the dominant scattering mechanisms in all investigated temperature range. Other scattering mechanisms give negligibly small contributions. A difference between the theoretical curve and experimental data is observed in the low temperature region, too. The probable cause is the same as in the case of ZnCdTe.

To conclude, the charge carrier scattering processes on various lattice defects in the $Zn_xCd_{1-x}Te$ and $Zn_xHg_{1-x}Te$ solid solutions have been considered basing on the short-range principle. A rather well agreement between the theory and experimental data within the investigated temperature range has been established.

References

1. R.B.James, T.E.Schlesinger, J.Lund, M.Schieber, in: Semiconductors for Room Temperature Nuclear Detector Applications: Semiconductors and Semimetals, Academic Press, New York (1995), Vol.43, p.335.
2. R.Triboulet, G.Neu, B.Fotouhi, *J. Cryst. Growth*, **65**, 262 (1983).
3. Y.Eisen, A.Shor, *J. Cryst. Growth*, **184/185**, 1302 (1998).

4. G.A.Gamal, M.Abou Zied, A.A.Ebnalwaled, *Physica B*, **393**, 285 (2007).
5. M.C.Veale, P.J.Sellin, A.Lohstroh et al., *Nucl. Instr. Meth. Phys. Res. A*, **576**, 90 (2007).
6. R.Triboulet, A.Lasbley, B.Toulouse et al., *J. Cryst. Growth*, **79**, 695 (1986).
7. K.Jozwikowski, A.Rogalski, *Infrared Phys.*, **28**, 101 (1988).
8. S.Rolland, K.Karrari, R.Granger et al., *Semicond. Sci. Technol.*, **14**, 335 (1999).
9. R.Granger, C.M.Pelletier, *J. Cryst. Growth*, **138**, 486 (1994).
10. Yi-Gao Sha, Ching-Hua Su, S.L.Lehoczky, *J. Appl. Phys.*, **81**, 2245 (1997).
11. O.P.Malyk, *Mater. Sci. &Eng.*, **B 129**, 161 (2006).
12. O.P.Malyk, *Phys. Stat. Solidi(c)*, **6**, 586 (2009).
13. J.J.Dubowski, *Phys. Stat. Solidi (b)*, **85**, 663 (1978).
14. O.P.Malyk, *WSEAS Trans. Math.*, **3**, 354 (2004).
15. S.Yamada, *J. Phys. Soc. Japan*, **15**, 1940 (1960).
16. M.Aven, B.Segall, *Phys. Rev.*, **130**, 81 (1963).

Локальна взаємодія носія заряду з дефектами гратки у твердих розчинах ZnCdTe та ZnHgTe

О.П.Малик

Розглянуто процеси розсіяння носія заряду на близькодіючому потенціалі, викликаному взаємодією з полярним та неполярним оптичними фононами, п'єзоелектричними та акустичними фононами, статичною деформацією, нейтральними та іонізованими домішками в $Zn_xCd_{1-x}Te$ ($0 \le x \le 1$) та $Zn_xHg_{1-x}Te$ ($x = 0.15$). Розраховано температурні залежності рухливості носія заряду в інтервалі температур 50–360 K.